Advances in River Sediment Research – Fukuoka et al. (eds)
© 2013 Taylor & Francis Group, London, ISBN 978-1-138-00062-9

A new method for measuring and calculating flows and bed forms around river banks

M. Koshiishi
Graduate School of Science and Engineering, Chuo University, Tokyo, Japan

T. Uchida & S. Fukuoka
Research and Development Initiative, Chuo University, Tokyo, Japan

ABSTRACT: Three-dimensional velocity distributions and bed-forms were measured around flow attacking zones in the experimental meandering channel in the Jyoganji River by using the Acoustic Doppler Current Profiler (ADCP). This paper presented a measuring method for accurate velocity and bed profiles using individual beam data for current profiles. We proposed a numerical analysis method for the local three-dimensional flow configuration around the revetment using bottom velocity computation method without the shallow water assumption. We validated the accuracy of new analytical method through the comparison with velocity distributions measured by the experiment. Results demonstrated that combined use of the measuring and calculating method presented here was useful to understand three-dimensional flows around structures.

1 INTRODUCTION

Revetments were constructed to prevent the erosion against natural banks, but they also caused severe bed scouring along revetments (Osada et al., 2007). It is necessary for a reliable bank protection to reveal flow configurations and to develop a calculation method of local flows around river structures.

The recent advances in computational technologies and numerical method make possible to investigate effects of the length and orientation angle of spur dikes on surrounding flows (e.g., Halting et al., 2007) and to reproduce the main features of bed scouring (e.g., Duc & Rodi, 2008). However, most applications of three-dimensional analysis are limited to the small scale phenomena in the laboratory channels. As it stands now, it is safe to say that three-dimensional numerical methods are rather hard to apply to scour problems for actual flood in rivers. Because, flows attacking on revetments and resulting bed variations are influenced by the large scale phenomena such as the channel plan-form, water surface profiles, the discharge hydrograph, sand bars and so on. Then, a computational method for flows around structures, which can apply to flows in a long reach during a flood event, is required. The reliable measurement data for model verifications is also needed to develop a numerical model for actual flow phenomena in rivers.

Uchida & Fukuoka (2012) have developed a new depth integrated model without the assumption of the shallow water flow to capture three-dimensional flows and bed variations around structures: general Bottom Velocity Computation (BVC) method. To understand flow configurations attacking on revetments and to obtain detailed three-dimensional velocity data for verifications of numerical models, Koshiishi et al. (2012a) proposed the new method for measuring three-dimensional velocity profiles around structures using Acoustic Doppler Current Profiler (ADCP). We applied the method to the field experiment with the actual scale conducted in the Jyogaji River. But problems in measurements of flows and bed-forms still remain; bottom tracking beam data for measuring river bed-forms in ADCP could not be collected at many points. Some studies have suggested that errors in measuring bed-forms by ADCP could be brought by side banks in the cross-section, resulting from averaging beam data from four transducers in different directions (Gunawan et al., 2010, Nihei et al., 2008).

This paper has twofold purposes. First, we develop a new method for measuring three-dimensional flows and river bed-forms using ADCP. Second, we apply the general BVC method without the assumption of the shallow water flow to the field experiment in the Jyoganji River, and validate its applicability to flow attacking zones around revetments.

2 A NEW METHOD FOR MEASURING FLOWS AND BED-FORMS USING ADCP

In this section, we develop the integrated measurement method of flows and river bed-forms using the individual current beam data of the ADCP. And, we validate the accuracy of the method by the field experiment in the Jyoganji River in 2011. One of the purposes of the experiment was to investigate characteristics of erosion and bed scouring beside revetments (Koikeda et al., 2012). The other was to obtain the detailed data of the actual flood scale to develop and validate the computation method for flow and bed scouring in flow attacking areas. Figure 1 and Table 1 show the plan view of the experimental channel and experimental conditions, respectively. The experiment was conducted in a compound meandering channel with two vertical revetment walls: flow attacking zone 1 and 2 in Figure 1. Figure 2 shows the picture of the velocity measurements at the flow attacking zone 1. The three-dimensional components of velocities and bed-forms by means of ADCP were measured around the flow attacking zone 1. The time and the cross-sectional space intervals are 10.0 s and 0.1 m, respectively. The draft of the ADCP was decided to avoid the effects of bubbles, because the velocity is very high around 2.5 m/s. Therefore, velocity data couldn't be collected in the range of about 0.4 m depth from water surface. In the two cross-sections, velocities to 0.15 m from water surface are measured by the electromagnetic current meter. Velocity variations around water surface induced by the draft of ADCP were investigated by Muller et al. (2007). For their experimental case of mean velocity 2.0 m/s, the velocity was reduced by about 5 percent at the distance 0.20 m from transducer of ADCP. Effects of the ADCP's draft in this experiment were negligibly small, because we measured velocity profile under 0.22 m from the transducer of ADCP.

2.1 *The method for measuring three-dimensional flow configurations (Koshiishi et al., 2012a)*

Figure 3 shows the concept of the conventional ADCP method. The conventional ADCP method gives three-dimensional velocities v_x, v_y, v_z in Equation 1 by using four individual beam data v_1–v_4 (Teledyne RD Instruments, 2006).

$$v_x = \frac{-v_3 + v_4}{2\sin\theta}, \quad v_y = \frac{-v_1 + v_2}{2\sin\theta},$$
$$v_z = \left(\frac{v_1 + v_2}{2\cos\theta} + \frac{v_3 + v_4}{2\cos\theta}\right)\Big/2 \tag{1}$$

However, the conventional method cannot give accurate velocity distributions of flows with local velocity gradients and deep water depth, because of velocity variations within the focus spot L which expands towards the vertical direction by the angle of 20 degrees. So in this method, lateral and vertical velocity at any point are calculated by Equation 2 using superimposing spatially-interpolated individual beam data v_{1in}, v_{2in} which are measured continuously in lateral direction and averaged over time as shown in Figure 4. For the above method, we introduce the assumption of

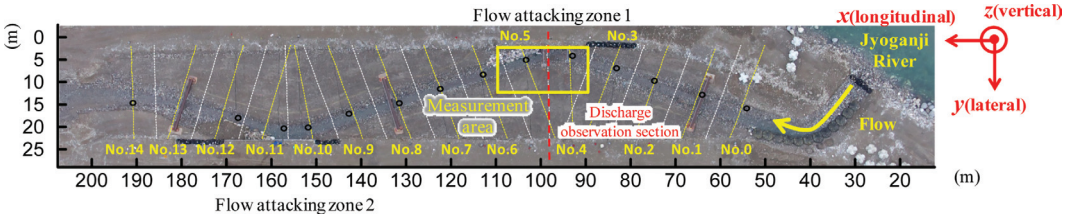

Figure 1. Plan view of the experimental channel.

Table 1. Experimental conditions.

	Mean velocity [m/s]	Water width [m]	Mean depth [m]	Froude number	Discharge [m³/s]
Main channel	1.4	5.0	0.7	0.53	5.2
Flood plane	0.8	15.0	0.2	0.57	2.4
Total channel	1.1	20.0	0.3	0.64	7.6

Channel length: 170.0 m. Channel slope: 1/200.

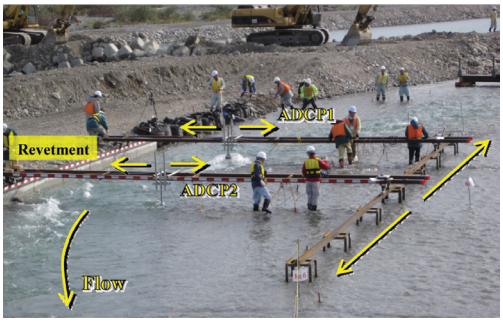

Figure 2. Picture of the measurements around the flow attacking zone 1.

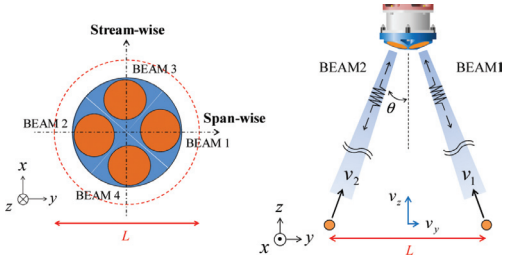

Figure 3. Concept of the conventional ADCP method.

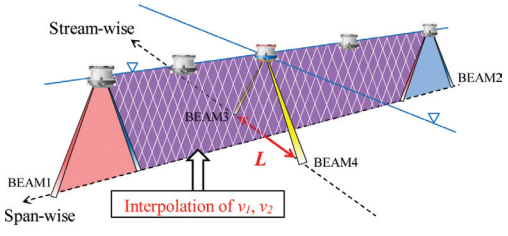

Figure 4. Concept of the present ADCP method.

little variation in temporal mean velocity during the measurement.

$$v_y = \frac{-v_{1in} + v_{2in}}{2\sin\theta}, \quad v_z = \frac{v_{1in} + v_{2in}}{2\cos\theta} \tag{2}$$

In this paper, it is assumed that variations in stream-wise velocity component v_x are negligibly-small compared with those of the lateral and vertical direction; only the stream-wise velocity v_x is calculated by Equation 1 using in similar way to the conventional method. Koshiishi et al. (2012a) have shown that the method could measure concentrated flows in front of the revetment with accuracy. Especially in the vicinity of bed surface, the measuring method performed the improved accuracy compared to the conventional ADCP method with averaged four beam data.

2.2 *A new method for measuring river bed-forms using current profile data of ADCP*

ADCP transmits bottom tracking beam for bed-form mappings in addition to the current beam. In the measurement towing ADCP, absolute velocities are calculated by using relative velocity of the water and the ground (i.e., ship velocity) measured by bottom tracking beam (Gunawan et al., 2010, Nihei et al., 2008, Teledyne RD Instruments, 2006). However, bottom tracking beam data are often lost or erroneous, because it is necessary to prepare applicable values of some parameters such as backscatter intensity (dB) and pulse-to-pulse correlation (count) for capturing the river bed. These values would vary depending on observation conditions in rivers. In the Jyoganji River field experiment with cobbles on the bed surface, bottom tracking data could not be obtained in a lot of points due to the use of the factory-default setting for those parameters. In the present measuring method, velocity and bed profiles are analyzed by the post-processing of individual beam data for current profiling by ADCP. Figures 5 and 6 show

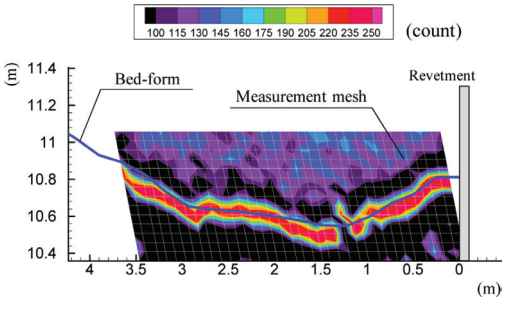

Figure 5. Distributions of correlation values and the bed-form observed by the total station.

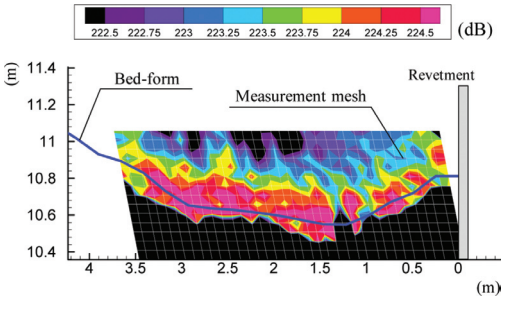

Figure 6. Distributions of intensity values and the bed-form observed by the total station.

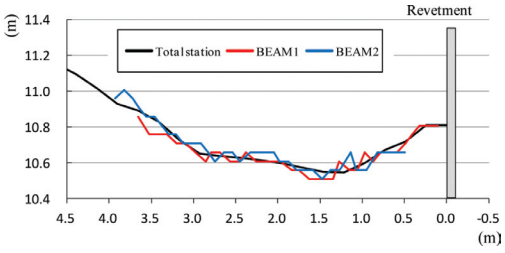

Figure 7. Bed-forms estimated by present method and observed by total station.

contours of the correlation and the intensity measured continuously in the lateral-section. The river bed-forms observed by the total station are also shown in their figures as blue solid lines. The intensity values had varied quite a bit through measurement sections or measurement points. On the other hand, the correlation values show significant changes at the vicinity of the bed surface in contrast to those of the intensity values. For these reasons, this method evaluates river bed-forms by using the correlation values. Figure 7 shows river bed-forms measured by the total station, and estimate values of the bed surface by BEAM1 and BEAM2 that are defined as the bed surface at 210 count of the correlation values. While estimated bed profiles have an error of up to 0.1 m compared to the total station because of maximum particle diameter of 0.1 m on the bed surface and use of 0.05 m depth cells, this method reproduces bed-forms with practical accuracy.

As above discussions, the new method by using individual current beam data can provide us accurate bed-forms data in addition to detail data of velocity distributions. So, the method makes it possible to obtain effective data of scouring problems.

3 GENERAL BOTTOM VELOCITY COMPUTATION METHOD WITHOUT SHALLOW WATER ASSUMPTION

Figure 8 shows the concept of the bottom velocity computation method. In this method, the bottom level z_b on the thin vortex layer over the actual bed z_0 ($z_b = z_0 + \delta z_b$, $\delta z_b \fallingdotseq 0.05\,h$, h: water depth) is defined, and flows between the bottom and the water surface are calculated. The thickness of the bottom layer δz_b is decided to give the relationship between bottom velocity and shear velocity by Equation 3.

$$\frac{u_b}{u_*} = \frac{1}{\kappa}\ln\left(\frac{\delta z_b + a k_s}{k_s}\right) + 8.5 \qquad (3)$$

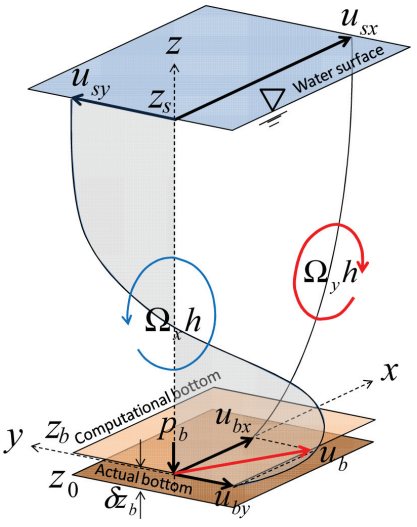

Figure 8. Concept of the bottom velocity computation method.

Here, $u_b^2 = u_{bi}^2$, u_{bi}: bottom velocity, u_*: shear velocity, k_s: equivalent roughness height, a: coefficient for the origin height of the log low. The bottom velocity is obtained in the Equation 4, depth-integrating horizontal vorticity.

$$u_{bi} = u_{si} - \varepsilon_{ij3}\Omega_j h - \left(\frac{\partial Wh}{\partial x_i} - w_s\frac{\partial z_s}{\partial x_i} + w_b\frac{\partial z_b}{\partial x_i}\right) \qquad (4)$$

Here, $i,j = 1,2(x,y)$, u_{si}: water surface velocity, Ω_j: depth averaged vorticity, W: depth averaged vertical velocity, z_s: water surface level, z_b: bottom level, w_s, w_b: vertical velocity on water surface and bottom. The vertical distribution of velocity is described by Equation 5.

$$u'_i = u_i - U_i = \Delta u_i\left(12\eta^3 - 12\eta^2 + 1\right) - \delta u_i\left(4\eta^3 - 3\eta^2\right) \qquad (5)$$

Here, U_i: depth averaged velocity, Δu_i: $u_{si} - U_i$, δu_i: $u_{si} - u_{bi}$, $\eta = (z_s - z)/h$, z: vertical level. If the vertical scale was much smaller than the objective horizontal scale, the terms in parentheses of the Equation 3 could be omitted (shallow water assumption: Uchida & Fukuoka, 2011). Koshiishi et al. (2012b) applied the BVC method with the shallow water assumption to a river confluence. They provided that the method could reproduce characteristics of the secondary flow distributions and depth averaged flow field in the river confluence. However, at the objective domain in this study such as flow attacking zones along revetments, these terms

couldn't be neglected for following reasons. First, the vertical scale would be considered as the same range with the horizontal scale due to downward flows in front of revetments. Second, distributions of the pressure deviate from those of the hydrostatic pressure. Therefore, to obtain the bottom velocity in Equation 4 it is required to calculate the depth averaged vorticity equations (Eq. 9), the water surface velocity equations (Eq. 10) and the depth averaged vertical velocity equation (Eq. 11) in addition to the continuity equation (Eq. 6), the depth averaged momentum equations (Eq. 7) and the depth averaged turbulence energy transport equation (Eq. 8).

$$\frac{\partial h}{\partial t}+\frac{\partial U_j h}{\partial x_j}=0 \tag{6}$$

$$\rho\left(\frac{\partial U_i h}{\partial t}+\frac{\partial U_i U_j h}{\partial x_j}\right)=-\rho g h\frac{\partial z_s}{\partial x_i}-\frac{\partial h dp_0}{\partial x_i} -dp_b\frac{\partial z_b}{\partial x_i}-\tau_{bi}+\frac{\partial h\tau_{ij}}{\partial x_j} \tag{7}$$

$$\frac{\partial k}{\partial t}+U_j\frac{\partial k}{\partial x_j}=\frac{1}{h}\frac{\partial}{\partial x_i}\left(\frac{\nu h}{\sigma_k}\frac{\partial k}{\partial x_i}\right)+P_k-\varepsilon \tag{8}$$

Here, τ_{bi}: bed shear stress, dp: pressure deviation from hydrostatic pressure distribution ($p=\rho g(z_s-z)+dp$), dp_0: depth averaged dp, dp_b: dp on bottom, τ_{ij}: horizontal shear stress due to turbulence ν_t S_{ij} and vertical distribution of velocity $\overline{u_i' u_j'}$, S_{ij}: depth averaged strain velocity, $\overline{u_i' u_j'}$: depth averaged $u_i' u_j'$ evaluated by the vertical distribution of velocity of quadratic curve (Eq. 5), ν: $\nu_m+\nu_t$, ν_t: eddy viscosity ($\nu_t=C_\mu k^2/\varepsilon$, $C_\mu=0.09$), ν_m: kinematic viscosity, k: depth averaged turbulence energy, P_k: production term, ε: dissipation term ($\varepsilon=C_\varepsilon k^{3/2}/\Delta$, $C_\varepsilon h/\Delta=1.7$).

$$\frac{\partial \Omega_i h}{\partial t}=ER_{\sigma i}+P_{\omega i}+\frac{\partial h D_{\omega ij}}{\partial x_j}$$

$$ER_{\sigma i}=u_{si}\omega_{s\sigma}-u_{bi}\omega_{b\sigma}$$

$$P_{\omega i}=C_{p\omega}\nu_{tb}(\omega_{bei}-\omega_{bi})/h,\quad C_{p\omega}=\kappa/\alpha,\quad \alpha=\kappa\sqrt{6}$$

$$D_{\omega ij}=-U_j\Omega_i+U_i\Omega_j+\overline{\omega' u'}_i-\overline{\omega' u'}_j+\frac{\nu_t}{\sigma_\omega}\frac{\partial \Omega_i}{\partial x_j}$$

$$\overline{\omega' u'}_i=\frac{\varepsilon_{ki3}}{h}\left(\frac{6}{5}\delta u_j\Delta u_k-\left(\frac{1}{5}\Delta u_j+\frac{1}{2}\delta u_j\right)\delta u_k\right) \tag{9}$$

Here, $\omega_{s\sigma}$ and $\omega_{b\sigma}$ are evaluated by the rotation of u_{si} and u_{bi}, ν_{tb}: eddy viscosity on bottom converted to depth averaged value, ω_{bei}: equilibrium vorticity on bottom calculated by the shear stress. The equation concerning a water surface velocity is derived from momentum equation in the very thin layer δz_s ($\to 0$) below the water surface.

$$\frac{\partial u_{si}}{\partial t}+u_{sj}\frac{\partial u_{si}}{\partial x_j}=-\left\{g-\left(\frac{\partial dp}{\partial z}\right)_{z=z_s}\right\}\frac{\partial z_s}{\partial x_i}+P_{si}$$

$$P_{si}=\frac{2\nu_t}{h^2}\left\{12\left(u_{sei}-u_{si}\right)-\left(3\delta u_i-6\Delta u_i\right)\right\} \tag{10}$$

Here, u_{sei}: $U_i+(\delta u_i-\Delta u_i)$. Production term P_{si} is only considered shear stress acting on undersurface of the very thin layer δz_s, because δz_s is defined as an infinitesimal layer. It is obtained by vertical distribution of horizontal velocity (Eq. 5), satisfying the constraint condition for uniform flow velocity distribution. Time variation in the depth integrated vertical velocity is calculated in Equation 11.

$$k_1\frac{\partial}{\partial x_j}\left(h^2\frac{\partial \phi}{\partial x_j}\right)+\phi^P-\phi=0 \tag{11}$$

Here, $k_1=1/20$, $\phi=(Wh)^{n+1}-(Wh)^n$, $\phi^P=(Wh)^P-(Wh)^n$, $(Wh)^n$: calculated Wh by the vertical distribution of velocity with $\delta u^p{}_i$, $\delta u^p{}_i$: calculated δu_i in Equation 3 with $(Wh)^n$, n: time step. Equation for bottom pressure (Eq. 12) is described by the depth averaged momentum equation in vertical direction without horizontal shear stress and unsteady terms.

$$\frac{\partial h W U_j}{\partial x_j}=\frac{dp_b}{\rho}-\tau_{bj}\frac{\partial z_b}{\partial x_j} \tag{12}$$

In this method, the vertical distribution of velocity (Eq. 5) is defined as cubic polynomial by using depth averaged velocity U_i, water surface velocity u_{si}, bottom velocity u_{bi} and assumption of non velocity gradient at water surface ($(\partial u/\partial z=0)_{z=zs}$). Correlation terms about vertical distributions of velocity and vorticity described by superscript bar in Equations 7, 9 and production terms in Equations 8–10 are calculated by using Equation 5. All governing equations are interrelated through these terms with the vertical distributions of velocity.

4 APPLICATION TO THE FIELD EXPERIMENT IN THE JYOGANJI RIVER

4.1 *Calculation setup*

In this section, we apply the general BVC method without the shallow water assumption to the field

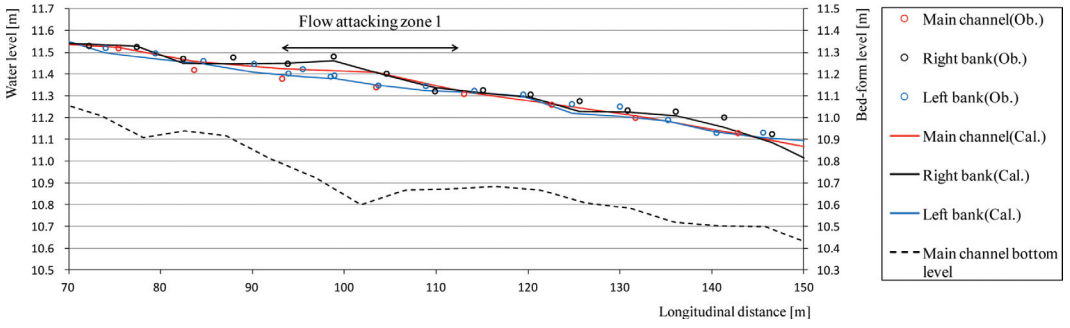

Figure 9. Comparison of water surface profiles.

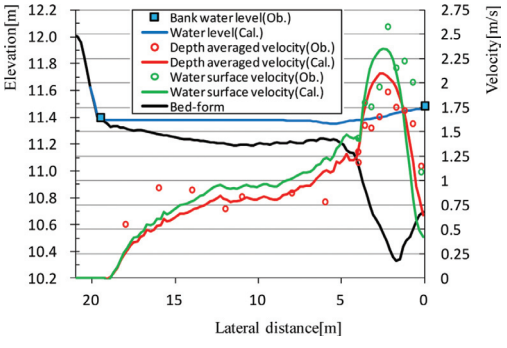

Figure 10. Water surface velocity, depth averaged velocity and bank water level at cross-section E.

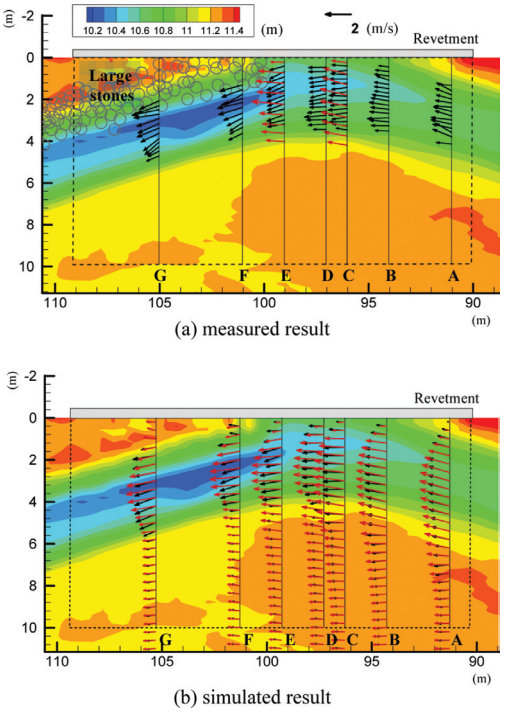

Figure 11. Comparisons of water surface and bottom velocity.

experiment in the Jyoganji River in order to validate its applicability to the large scale three-dimensional flow. The observed water surface profiles are used as boundary conditions of upstream and downstream, since they are considered to have higher accurate values than observed discharge (Fukuoka, 2005). The distributions of bed roughness on the main channel and the flood plane are determined to reproduce measured water surface profiles, discharge and velocity distributions depending on cobble diameter on the bed surface (ks = 0.2 m, 0.1 m, 0.25 m for x = 0–80 m, 80–120 m, 120–200 m from the inlet, respectively). The length and width of computational cells are 0.5 m and 0.25 m with Cartesian coordinate. The bed level data are set by using data observed by total station at intervals of 5.0 m. In the flow attacking zone 1, detailed observation results of bed-forms by the present ADCP method are used to complement them.

4.2 *Comparisons between measurement and analysis*

Figure 9 shows the comparison between measured and calculated water surface profiles. Figure 10 shows comparisons of the longitudinal components of the depth averaged velocity, water surface velocity and water level on both banks at cross-section E (see Fig. 11). While calculated water surface profiles are slightly lower than measured one downstream from 120 m, calculated values provide good agreements with measured values on both banks around flow attacking zone 1 (Fig. 9). However in the case of main channel profiles as shown in the red line and plots, calculated values are about 0.05 m higher than measured values

within the section of 82–110 m. This would be considered as follows. Measured water levels of the main channel were observed around interface between the main channel and the flood plane. In this area, there are complex momentum transports due to inflow from the flood plane to the main channel as shown in Figure 11. And, the large gradient of water surface in the span-wise direction is also induced by steep velocity variations as shown in Figure 10. Although calculated results reproduce

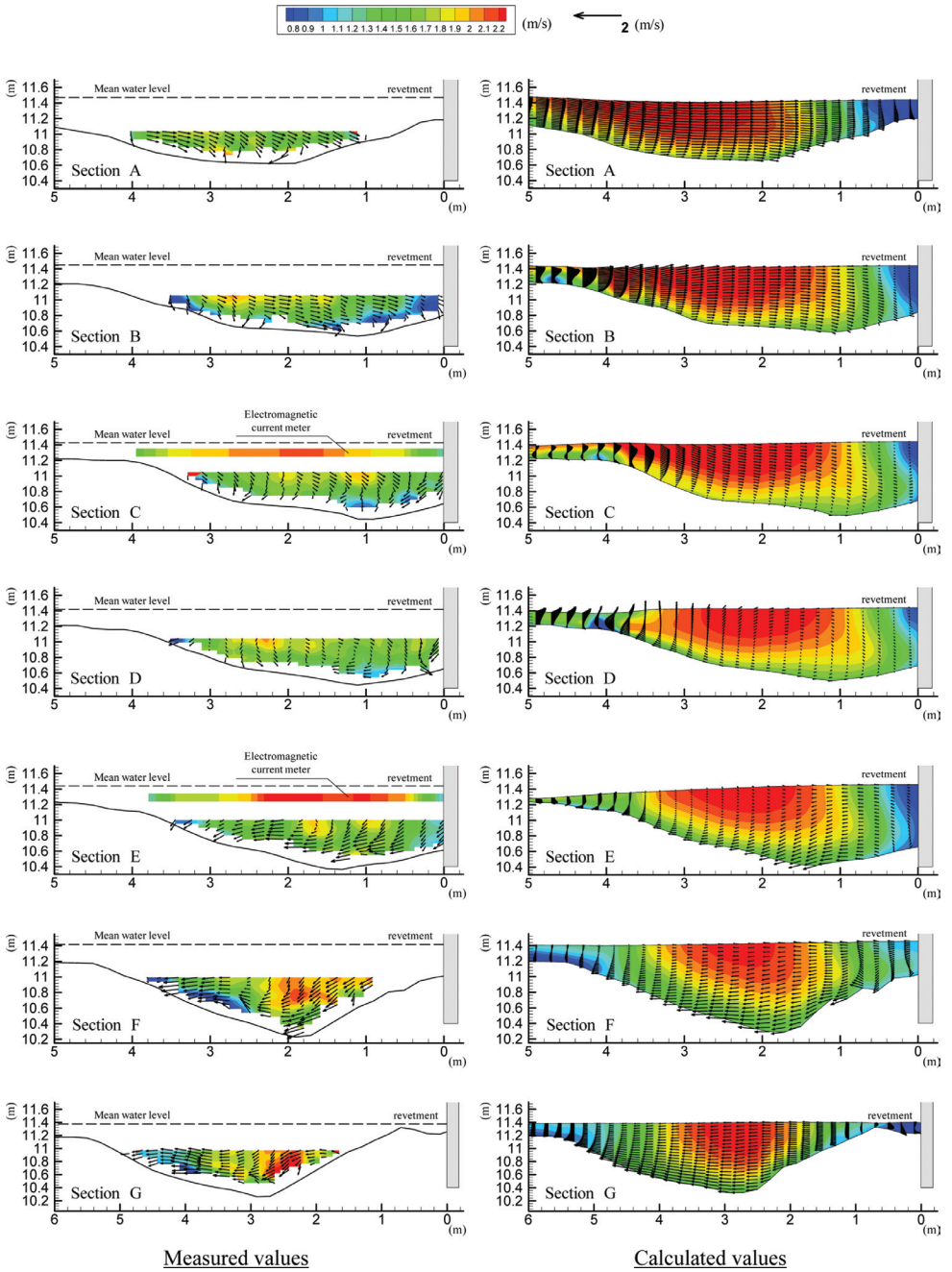

Figure 12. Comparison of primary flow contour and secondary flow vector.

characteristics of depth averaged and water surface velocity distributions, the calculated main stream doesn't sufficiently close to the revetment compared to measured results. Therefore, the location of low water surface level is considered to be different from the actual one. However, about 0.05 m difference of water level between the inner and the outer bank (Fig. 10, 0–5 m) is almost reproduced by the calculation (Fig. 9, 82–110 m). In Figure 11, black vectors and red vectors show bottom velocities and water surface velocities, respectively. Measured bottom velocities are defined as averaged velocities around 80 percent of depth and water surface velocities are the measurement values by the electromagnetic current meter at 0.15 m from the water surface. Figure 12 shows vertical distribution of velocity of the primary flow as contour and the secondary flow as vector at cross-sections A-G. In cross-sections C and E, primary flow contours also show measured results of electromagnetic current meter around water surface. According to the measurement results, the secondary flow develops around cross-section C-F with the downward flow along the revetment at right bank (Figs. 11 and 12). The momentum of the primary flow is transported to the bottom of the outer bank from the surface of the inner bank by the secondary flow, and the high velocity region extends to the vicinity of the bottom at the cross-section F (Fig. 12, cross-section F). In the calculation, intensity of the secondary flow is lower than measured results, and the high velocity region around the bottom at the cross-section F is not reproduced well. The reasons are discussed below. In this field experiment, the primary flow increases rapidly in vertical direction around water surface, as indicated from cross-section C and E of Figure 12. It is assumed that that large span-wise vorticity with the approaching flow would be converted to the stream wise vorticity due to the flow deflection induced by the revetment with the channel bend. However, the calculated span-wise vorticity with the approaching flow is low: the difference between water surface and bottom velocity of primary flow in the calculated results is smaller than that of the measurement as shown in Figures 10–12. Therefore, the intensity of secondary flow and momentum transports are underestimated. The possible causes of the above discrepancy between calculated and measured results are below. First, the approaching flow which is the boundary condition of the flow attacking zone 1 doesn't be calculated sufficiently. It depends on the given calculation condition such as bed roughness coefficients in the main channel and flood plain with diverse grain size distribution, bed-forms around inlet upstream cross-section No. 0 (i.e., angle and width, see Fig. 1). Second, the model parameters related to vorticity intensity are not correct for calculating large scale phenomena. Although, the general BVC method have been verified by simplified laboratory experiments, the flow conditions in the vicinity of bottom are more complex for flows on gravel bed rivers. Third, the present model employed the linear eddy viscosity model with only the turbulence energy transport equation by using dissipation term related with water depth. Although these are problems to be solved, calculated results provide explanation for the measured characteristics of the secondary flow and the momentum transport in the field experiment located on the complicated channel alignment. Especially, at the place where the clockwise secondary flow is occurred at cross-section E-F, the calculation provides downward flow around 3–4 m, while the absolute value is low. The calculation results around E-F show the interactions between the flow from the flood plane to the main channel and the flow the outer bank to the inner bank formed by secondary flow. The results demonstrate that combined use of the new measuring and calculating method is reliable to evaluate three-dimensional flows around structures.

5 CONCLUSIONS

We developed the new method for measuring three-dimensional flow configurations and river bed-forms using ADCP, and applied to the full scale experiment in the Jyoganji River. And, the general Bottom Velocity Computation method without the shallow water assumption was validated using the experiment data.

The new method using individual current profile data of ADCP makes it possible to measure detailed velocity distributions and river bed-forms around structures.

The general BVC method reproduces characteristics of the secondary flow and the momentum transport in the flow attacking zones along revetments.

Complex three-dimensional flow fields and severe scouring are expected to be solved by combined use of the measuring and the calculating methods in addition to observations of temporal water surface profiles and cross-sectional forms.

REFERENCES

Duc, B.M. & Rodi, W. 2008. Numerical simulation of contraction scour in an open laboratory channel, *Journal of Hydraulic Engineering*, *April*: 367–377.

Fukuoka, S. 2005. *Flood hydraulics and river channel design*, Tokyo: Morikita publishing company.

Gunawan, B., Sterling, M., Tang, X. & Knight, D.W. 2010. Measuring and modeling flow structures in a small river, *River Flow*: 179–186.

Halting, T.W., Biron, P.M. & Lapointe, M.F. 2007. Predicting equilibrium scour-hole geometry near angled stream deflectors using a three-dimensional numerical flow model, *Journal of Hydraulic Engineering*, *August*: 983–988.

Koikeda, S., Ishii, A., Iwai, H., Ishikawa, T. & Fukuoka, S. 2012. Nature friendly bank protection works using sandbars with boulders in the Jyoganji river, *Advances in River Engineering* 18: 233–238. JSCE.

Koshiishi, M., Uchida, T. & Fukuoka, S. 2012a. A new method for measuring local flows around river bank using ADCP, *The 10th Int. Conf. on Hydroscience and Engineering (ICHE-2012)*, *4–8 November*.

Koshiishi, M., Uchida, T. & Fukuoka, S. 2012b. A bottom velocity computation method with water surface velocity equation for flows around river confluence, *Annual Journal of Hydraulic Engineering* 56: 835–840. JSCE.

Muller, D.S., Abad, J.D., Garcia, C.M., Gartner, J.W., Garcia, M.H. & Oberg, K.A. 2007. Errors in acoustic Doppler profiler velocity measurements caused by flow disturbance, *Journal of Hydraulic Engineering*, *December*: 1411–1420.

Nihei, Y., Irokawa, Y., Ide, K. & Takamura, T. 2008. Study on river-discharge measurements using acoustic Doppler current profilers, *Journal of Hydraulic, Coastal and Environmental Engineering* 64(2): 99–114. JSCE.

Osada, K., Abe, T. & Fukuoka, S. 2007. Formation mechanism of channels developing along the low water revetment in gravel bed rivers, *Advances in River Engineering* 13: 321–326. JSCE.

Teledyne RD Instruments 2006. *Acoustic Doppler current profiler principles of operation a practical primer, December.*

Uchida, T. & Fukuoka, S. 2011. A bottom velocity computation method for estimating bed variation in a channel with submerged groins, *Journal of JSCE* B1–67(1): 16–29.

Uchida, T. & Fukuoka, S. 2012. Bottom velocity computation method by depth integrated model without shallow water assumption, *Annual Journal of Hydraulic Engineering* 56: 1225–1230. JSCE.